

Supporting information for

Flexible phosphonium and sulfonate pair-to-pair self-assembled ionic organic single crystals for iodine capture

Mingxia Sun ^{a, b}, Jia Chen ^{*, a, b}, Ting Zhang ^a, Wei Xu ^{a, b}, Jing He ^{a, b}, Yunyun Zhang ^{a, b}, Huifeng Liu ^a, Shuang Zhang ^a, Juanjuan Wang ^a, Xin Li ^a, Yali Yang ^a, Hongdeng Qiu ^{*, a, b, c}

AUTHOR ADDRESS

^a CAS Key Laboratory of Chemistry of Northwestern Plant Resources and Key Laboratory for Natural Medicine of Gansu Province, Lanzhou Institute of Chemical Physics, Chinese Academy of Sciences, Lanzhou 730000, China

^b University of Chinese Academy of Sciences, Beijing 100049, China

^c Key Laboratory of Rare Earths, Ganjiang Innovation Academy, Chinese Academy of Sciences, Ganzhou 341000, China

* E-mail: jiachen@licp.cas.cn (J. Chen); hdqiu@licp.cas.cn (H. Qiu).

CONTENT

Reagent and apparatus.....	S4
Details of adsorption performance of iodine in iodine-cyclohexane	S5
Details of adsorption performance of iodine vapor	S5
Details of DFT calculations.....	S6
Figure S1. Schematic diagram of plane angle of benzene rings of PEBT and PBBT in four IOCs of (a) PEBT-NDS, (b) PEBT-PTS, (c) PBBT-PTS, (d) PBBT-BDS.....	S7
Figure S2. Schematic diagram of bond angle of alkyl chain of PEBT and PBBT in four IOCs of (a) PEBT-NDS, (b) PEBT-PTS, (c) PBBT-PTS, (d) PBBT-BDS.....	S8
Figure S3. Schematic diagram of topological structure of four IOCs of (a) PEBT-NDS, (b) PEBT-PTS, (c) PBBT-PTS, (d) PBBT-BDS.....	S9
Figure S4. Schematic diagram of ionic bond length of four IOCs of (a) PEBT-NDS, (b) PEBT-PTS, (c) PBBT-PTS, (d) PBBT-BDS.....	S10
Figure S5. TGA curve of four IOCs of (a) PEBT-NDS, (b) PEBT-PTS, (c) PBBT-PTS, (d) PBBT-BDS.....	S11
Figure S6. Standard curve of iodine concentration and absorbance in iodine-cyclohexan.....	S12
Figure S7. UV-Vis absorption curves of four IOCs in iodine-cyclohexane solution of (a, b) PEBT-NDS, (c, d) PEBT-PTS, (e, f) PBBT-PTS, (g, h) PBBT-BDS.....	S13
Figure S8. Adsorption of iodine in different concentrations of iodine-cyclohexane belongs to the time and corresponding dynamic fitting curve of (a) PEBT-NDS, (b) PEBT-PTS, (c) PBBT-PTS, (d) PBBT-BDS.....	S14
Figure S9. Photos of iodine-cyclohexane before and after adsorption of four IOCs of (a) PEBT-NDS, (b) PEBT-PTS, (c) PBBT-PTS, (d) PBBT-BDS.....	S15
Figure S10. Photos of four IOCs before and after iodine vapor adsorption of (a) PEBT-NDS, (b) PEBT-PTS, (c) PBBT-PTS, (d) PBBT-BDS.....	S16
Figure S11. Iodine adsorption in iodine vapor belongs to the time at 70 °C and their corresponding dynamic fitting curve of (a) PEBT-NDS, (b) PEBT-PTS, (c) PBBT-PTS, (d) PBBT-BDS.....	S17
Figure S12. Photos of four IOCs before and after iodine release in cyclohexane of (a) PEBT-NDS, (b) PEBT-PTS, (c) PBBT-PTS, (d) PBBT-BDS.....	S18
Figure S13. UV-Vis absorption curves of release in cyclohexane of (a) PEBT-NDS, (b) PEBT-PTS, (c) PBBT-PTS, (d) PBBT-BDS.....	S19
Figure S14. Photos of solubility of four IOCs in different solvents at 70 °C.....	S20
Figure S15. TGA curve of four IOCs before and after iodine adsorption of (a) PEBT-NDS, (b) PEBT-PTS, (c) PBBT-PTS, (d) PBBT-BDS.....	S21
Figure S16. UV-Vis absorption curves of four IOCs release in cyclohexane after iodine adsorption and I_3^- in water.	S22
Figure S17. XPS high-resolution spectrum of four IOCs before and after iodine adsorption of (a-c) PEBT-NDS, (d-f) PEBT-PTS, (g-i) PBBT-PTS, (j-l) PBBT-BDS.....	S23

Figure S18. XPS C high-resolution spectrum of four IOCs before and after iodine adsorption of (a) PEBT-NDS, (b) PEBT-PTS, (c) PBBT-PTS, (d) PBBT-BDS.....	S24
Figure S19. Element distribution mapping of four IOCs.	S25
Figure S20. Element distribution mapping of four IOCs after iodine adsorption.	S26
Figure S21. The lowest energy configurations, adsorption energies, and distances of (a-c) ring 1 of PEBT, ring 2 and O of NDS on I_2 sites, (d-f) ring 1 of PEBT, ring 2 and O of NDS on I_3^- sites, (g-h) ring 1 of PEBT, ring 2 and O of NDS on I_5^- sites.....	S27
Figure S22. Charge transfer diagrams of (a-c) ring 1 of PEBT, ring 2 and O of NDS on I_2 sites, (d-f) ring 1 of PEBT, ring 2, and O of NDS on I_3^- sites, (g-h) ring 1, ring 2, and O of NDS on I_5^- sites.	S28
Table S1. Preparation parameters of four IOCs.....	S29
Table S2. Unit cell packing of four IOCs.....	S30
Table S3. Plane angle of benzene rings of PEBT and PBBT in four IOCs.	S31
Table S4. Solubleness of four IOCs in different solvents at 70 °C.....	S32
Table S5. EDS data of four IOCs.....	S33
Table S6. EDS data of four IOCs after iodine adsorption.....	S34
Table S7. The distance between iodine atoms.....	S35
Table S8. Comparison with other reported iodine vapor adsorption properties.....	S36
References	S37

Reagent and apparatus

Phosphonium,1,1'-(1,2-ethanediyl)bis[1,1,1-triphenyl-, bromide](1:2) (PEBT, 98%) was purchased from Jiangsu Aikang Biomedical R&D Co., LTD (Nanjing, China); phosphonium,1,1'-(1,4-butanediyl)bis[1,1,1-triphenyl-bromide(1:2) (PBBT, 98%) and 1,5-naphthalenedisulfonic acid (NDS, 98%) were purchased from Shanghai Maclin Biochemical Technology Co., LTD (Shanghai, China); 1,3,6,8-pyrenetetrasulfonic acid, sodium salt(1:4) (PTS, 98%) and 4,4'-biphenyldisulfonic acid (BDS, 98%) were purchased from Shanghai Bide Pharmaceutical Technology Co., LTD. (Shanghai, China); Iodine purchased from Tokyo Chemical Industry Co., LTD. (Tokyo, Japan); Methanol (MeOH), cyclohexane, acetonitrile (MeCN), dimethyl formamide (DMF) and dimethylsulfoxide (DMSO) were purchased from Leanlon Bohua Pharmaceutical Chemistry Co., LTD. (Tianjin, China); Ultrapure water was produced by Milli-Q Purification Equipment (Millipore, Billerica, MA, USA).

The absorbance test of the I_2 was performed on UV-3600plus UV-Visible spectrophotometer (UV-Vis) (Shimadzu Corporation, Japan); The crystallographic data of the materials were analyzed by Smart APEX II X-ray single crystal diffractometer (Bruker Corporation, Germany) and XRD-6100 X-ray diffractometer (XRD, Shimadzu Corporation, Japan). The specific surface area and pore data of samples were tested by the Quantachrome EVO automatic specific surface and porosity analyzer (Canta Instruments, USA) and calculated with the Brunauer, Emmett, and Teller (BET) equation. The appearance was measured by ML31-M optical microscope (Guangzhou Mingmei Technology Co., LTD., China). Thermogravimetric analysis (TGA) of the material was tested using the STA449F3 synchronous thermal analyzer (NETZSCH Corporation, Germany) in an air atmosphere from 25 °C to 800 °C at a heating rate of 10 °C min⁻¹. The presence of elements on the surface of the material was analyzed on the ESCALAB 250Xi X-ray photoelectron spectrometer (Thermo Fisher Scientific, USA). Functional groups of materials were analyzed using a V70 Fourier transform infrared spectrometer (FT-IR, Bruker Corporation, Germany). The present form of iodine was tested on LabRAM HR Evolution micro confocal Raman spectrometer (HORIBA Jobin Yvon S.A.S., France). The element distribution was measured by energy dispersive spectrometer (EDS) on a SU8020 ultra-high resolution field emission scanning electron microscope (HITACHI, Japan).

Details of adsorption performance of iodine in iodine-cyclohexane

The sample iodine adsorption capacity is calculated according to the following equation (1):

$$Q_e = (C_0 - C_t) * V \text{ m}^{-1} \quad (1)$$

where Q_e represents the adsorption capacity of the sample at time t (mg g^{-1});

C_0 represents the initial concentration of iodine-cyclohexane solution (mg L^{-1});

C_t represents the concentration of iodine-cyclohexane solution (mg L^{-1}) at time t ;

V represents the volume (L) of the iodine-cyclohexane solution;

m represents the mass (g) of the IOCs.

Quasi-first-order kinetic model is fitted according to the following equation (2)¹

$$Q_t = Q_e * (1 - e^{-k_1 t}) \quad (2)$$

where Q_t represents the adsorption capacity at time t (mg g^{-1});

Q_e represents the adsorption capacity at equilibrium (mg g^{-1});

k_1 stands for quasi-first-order adsorption rate constant (min^{-1});

t is the adsorption time.

Quasi-second-order kinetic model is fitted according to the following equation (3)¹

$$Q_t = k_2 Q_e^2 t / (1 + k_2 Q_e t) \quad (3)$$

where Q_t represents the adsorption capacity at time t (mg g^{-1});

Q_e represents the adsorption capacity at equilibrium (mg g^{-1});

k_2 represents the quasi-second-order adsorption rate constant ($\text{g mg}^{-1} \text{ min}$);

t is the adsorption time.

Details of adsorption performance of iodine vapor

The sample iodine adsorption capacity is calculated according to the following equation (4)²

$$Q_t = 1000 * (m_2 - m_1) / m_1 \quad (4)$$

m_2 represents the adsorption capacity of the sample at time t (mg/g);

m_1 and m_2 represent the mass (g) of the IOCs before and after iodine adsorption, respectively.

Details of DFT calculations

The calculations were conducted using the Vienna ab initio simulation package (VASP v6.2.1)³⁻⁵ and the Perdew-Burke-Ernzerhof variant of the Generalized Gradient Approximation (GGA-PBE)⁶ functional was employed to obtain the exchange and correlation terms. To capture long-range vdW, the DFT-D3(BJ) approach by Grimme was utilized^{7, 8}.

For the structural refinement and associated computations, an energy threshold of 400 eV was applied, and a k-mesh 1*1*1 was adopted to ensure convergence of energy to 1*10⁻⁵ eV and forces to 0.02 eV Å⁻¹. The optimized lattice dimensions were determined to be 27.00 Å*27.00 Å*27.00 Å, with the angles α , β , and γ at 98.1°, 93.2°, and 107.0°, respectively. The charge density discrepancy, indicated by $\Delta\rho$, was computed by subtracting the charge density of the bare slab (ρ_{slab}) and the gas-phase molecules (ρ_{molecule}) from the total charge density of the slab with adsorbed molecules ($\rho_{\text{molecule@slab}}$), as expressed by the equation (5):

$$\Delta\rho = \rho_{\text{molecule@slab}} - \rho_{\text{slab}} - \rho_{\text{molecule}} \quad (5)$$

The analysis of charge transfer between the adsorbates and the surface was conducted through the application of Bader charge analysis.⁹

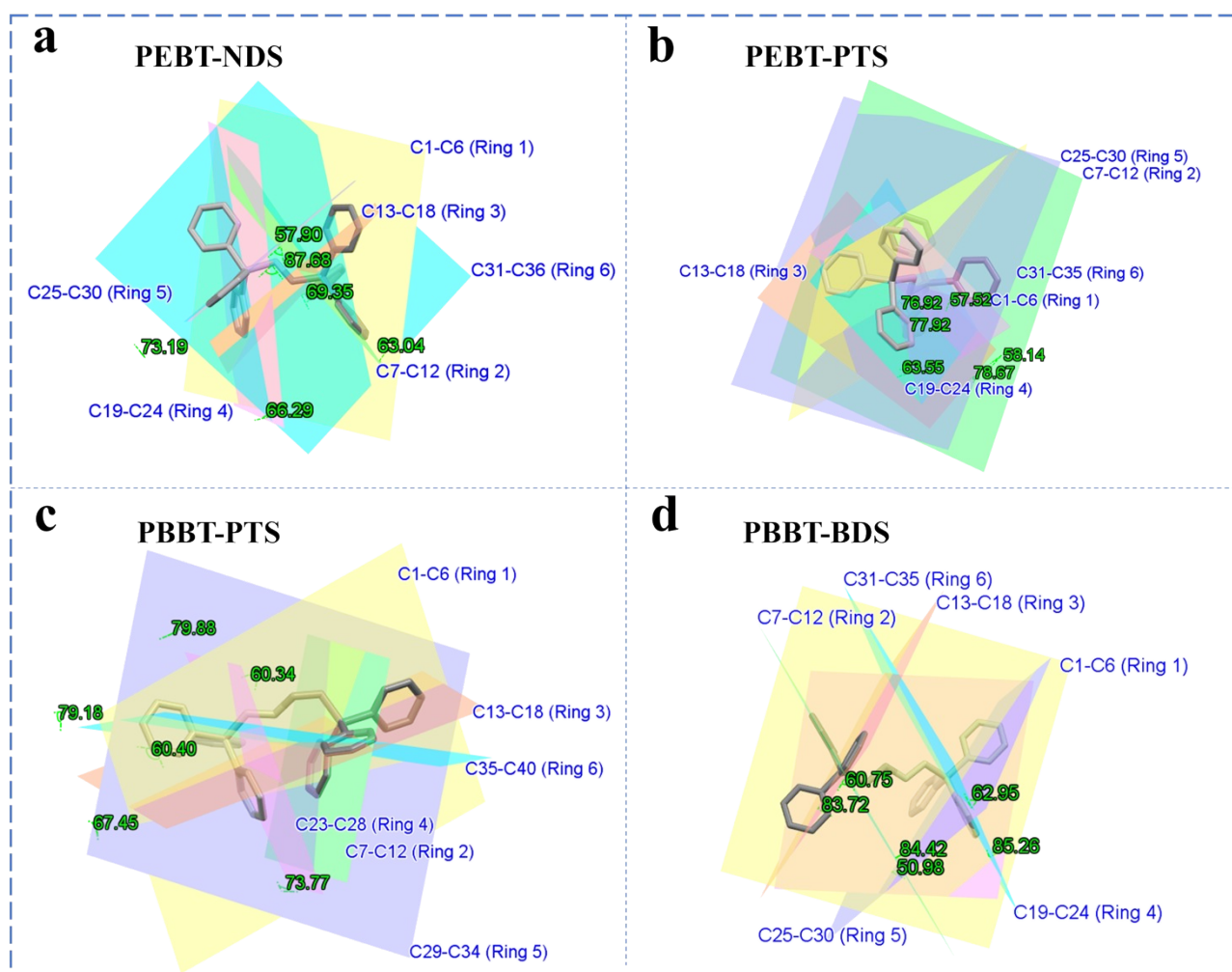


Figure S1. Schematic diagram of plane angle of benzene rings of PEBT and PBBT in four IOCs of (a) PEBT-NDS, (b) PEBT-PTS, (c) PBBT-PTS, (d) PBBT-BDS.

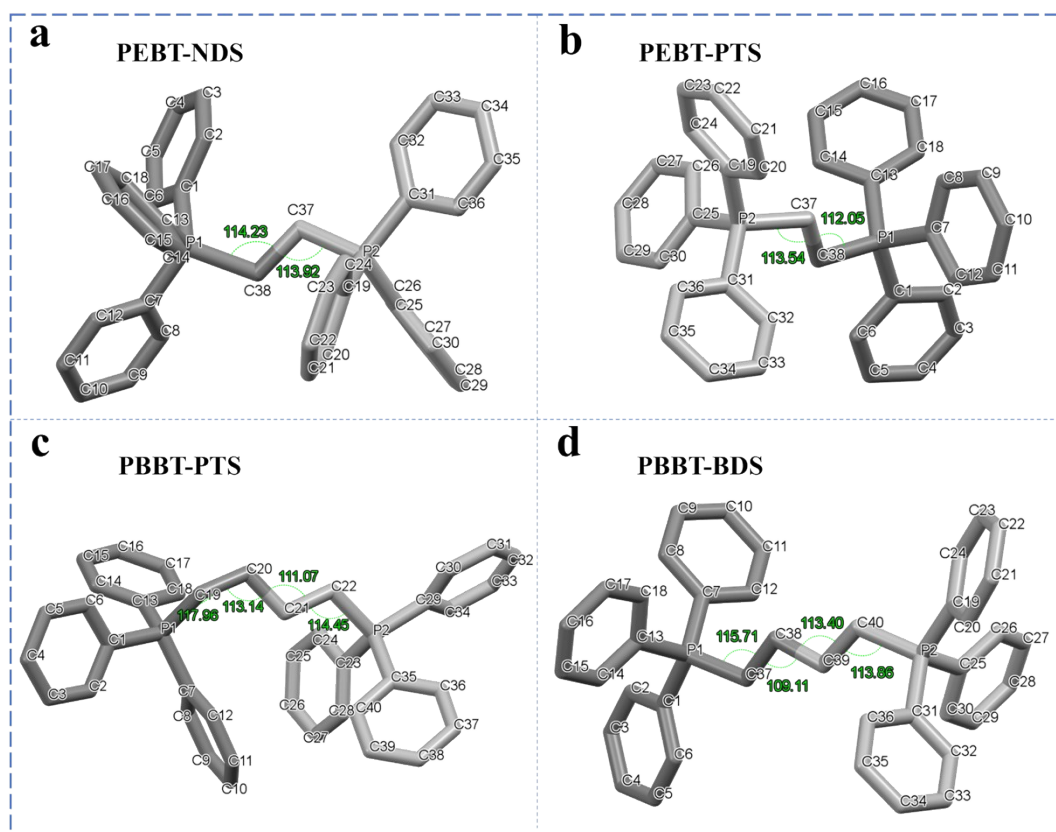


Figure S2. Schematic diagram of bond angle of alkyl chain of PEBT and PBBT in four IOCs of (a) PEBT-NDS, (b) PEBT-PTS, (c) PBBT-PTS, (d) PBBT-BDS.

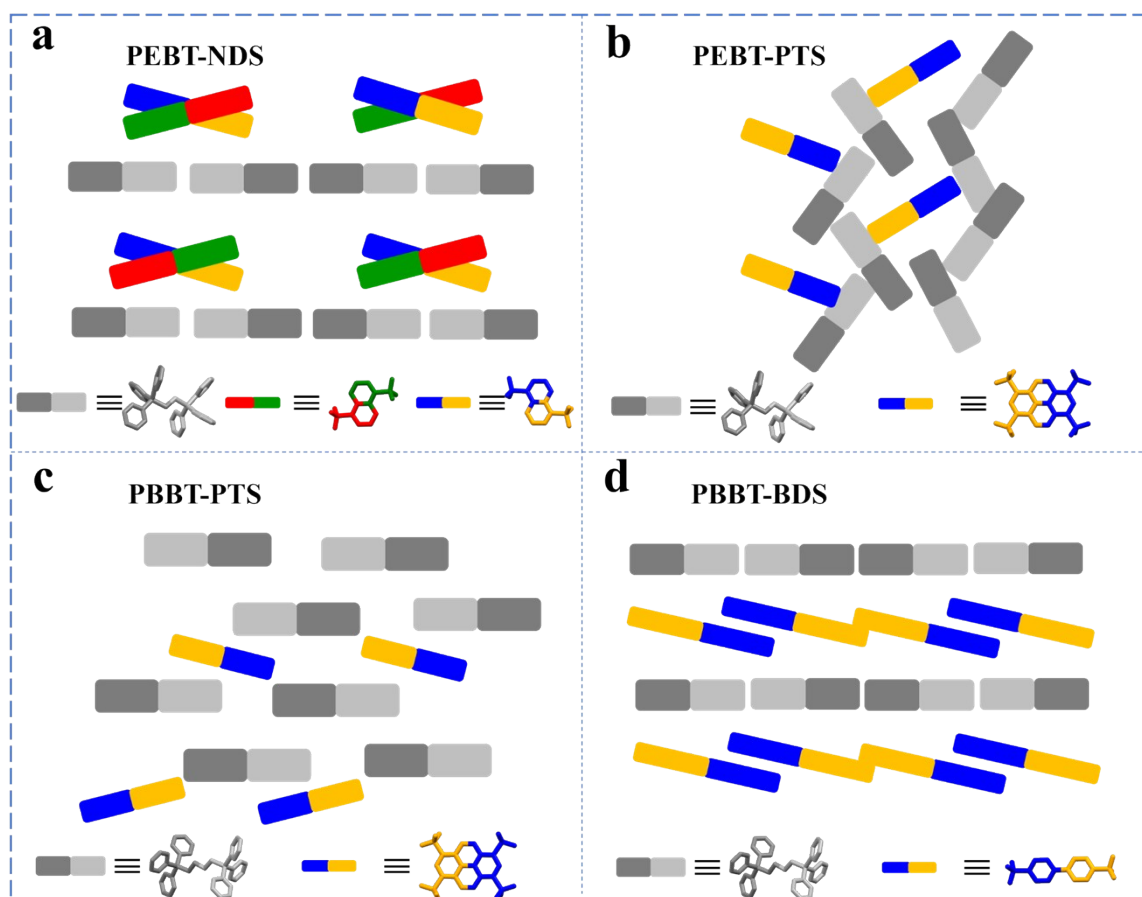


Figure S3. Schematic diagram of topological structure of four IOCs of (a) PEBT-NDS, (b) PEBT-PTS, (c) PBBT-PTS, (d) PBBT-BDS.

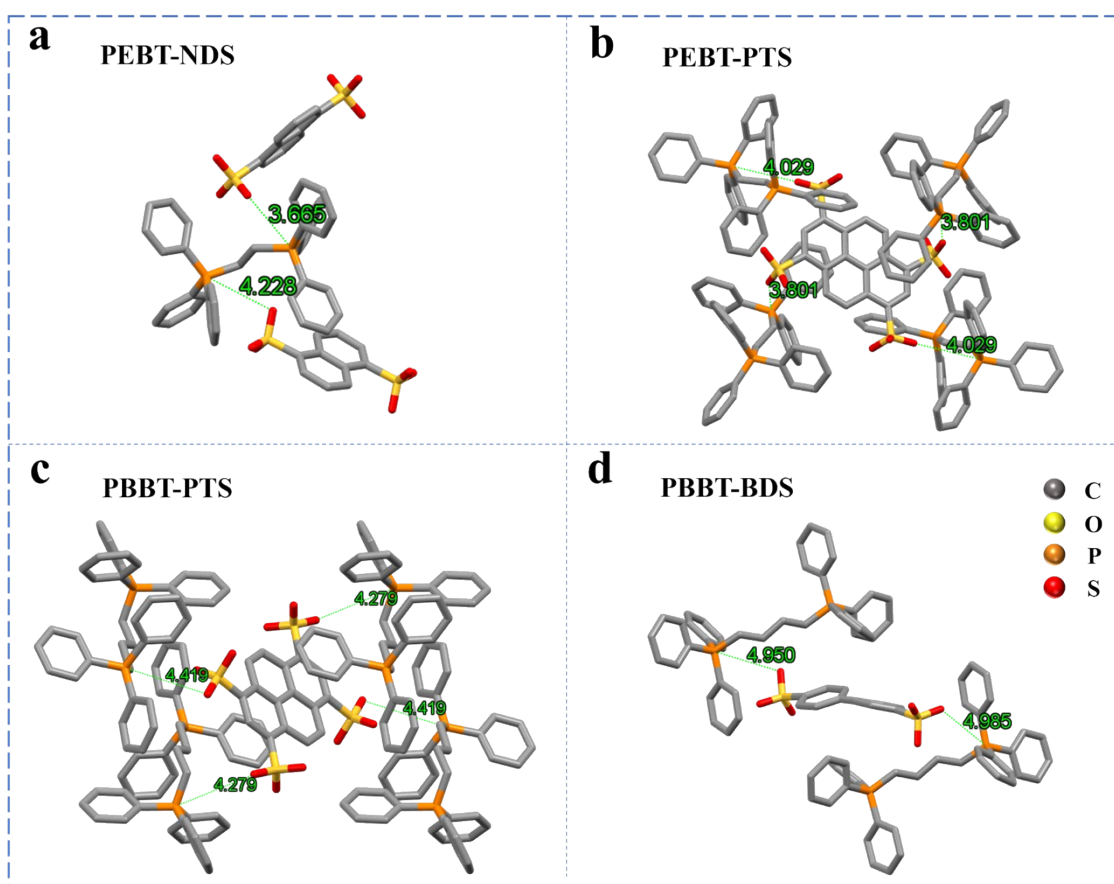


Figure S4. Schematic diagram of ionic bond length of four IOCs of (a) PEBT-NDS, (b) PEBT-PTS, (c) PBBT-PTS, (d) PBBT-BDS.

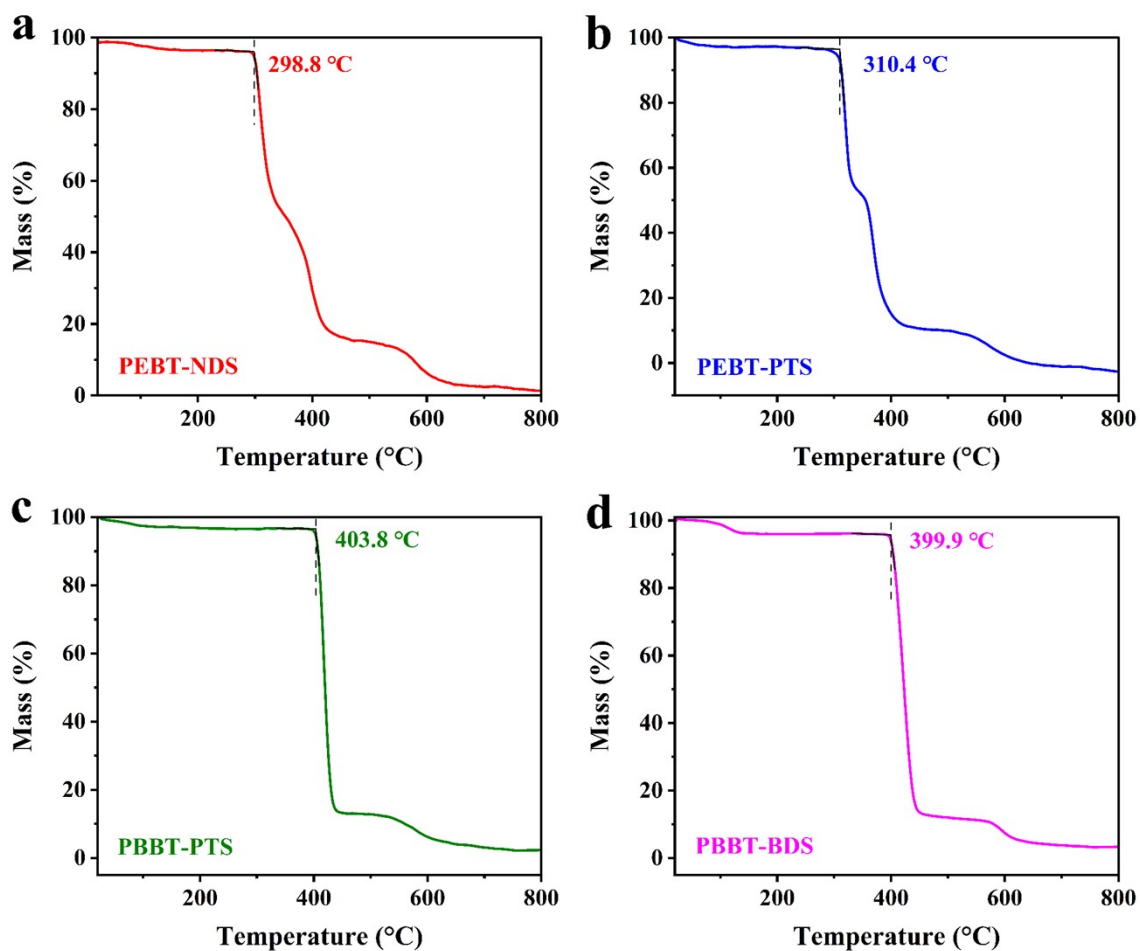


Figure S5. TGA curve of four IOCs of (a) PEBT-NDS, (b) PEBT-PTS, (c) PBBT-PTS, (d) PBBT-BDS.

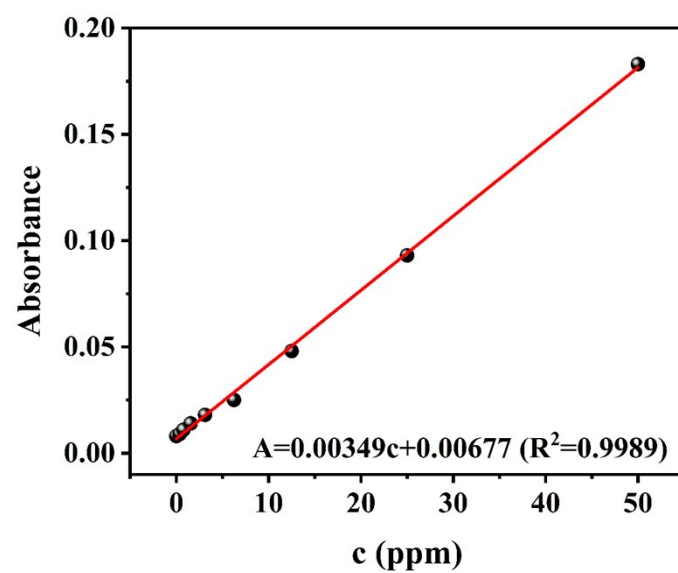


Figure S6. Standard curve of iodine concentration and absorbance in iodine-cyclohexane solution.

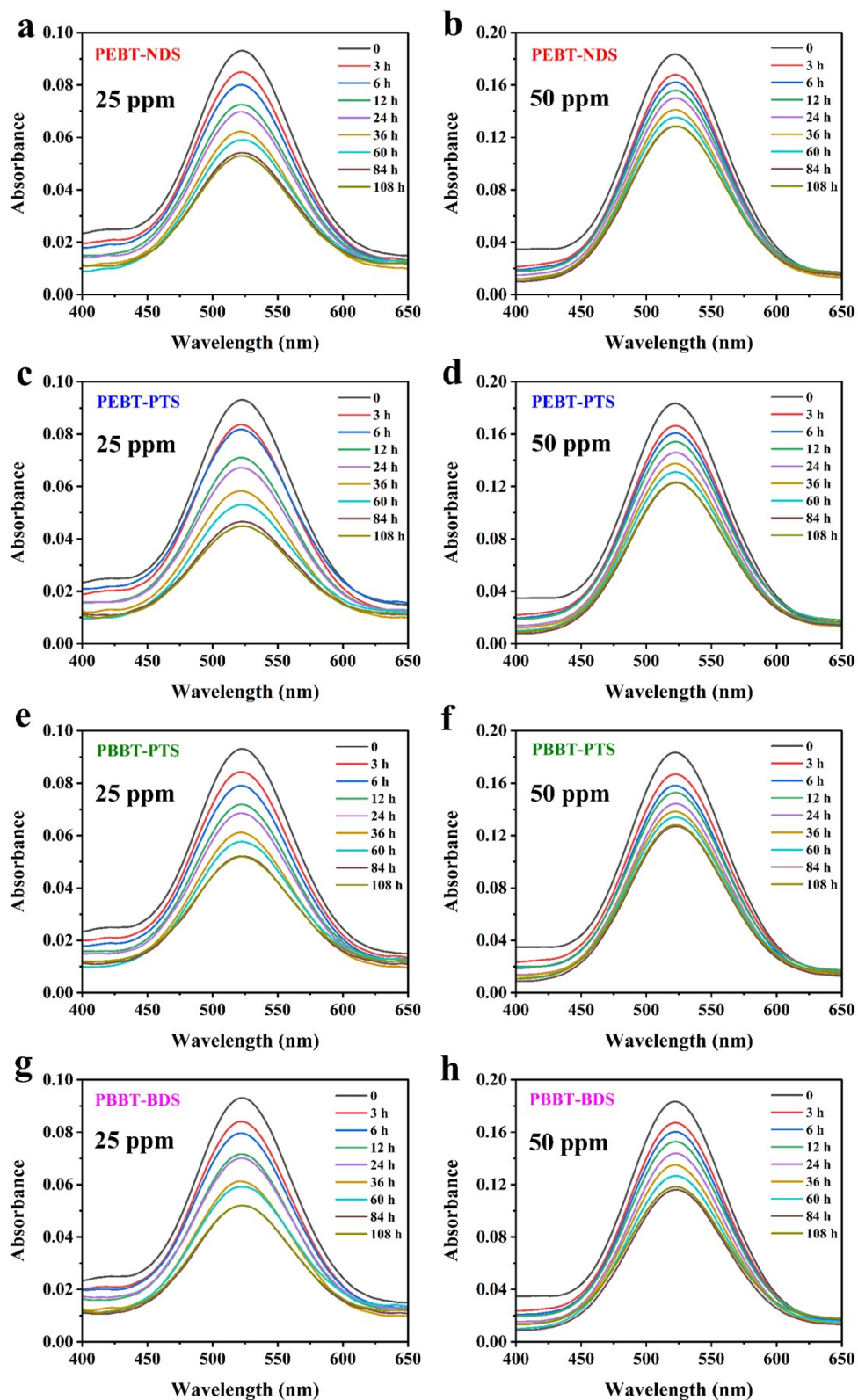


Figure S7. UV-Vis absorption curves of four IOCs in iodine-cyclohexane solution of (a, b) PEBT-NDS, (c, d) PEBT-PTS, (e, f) PBBT-PTS, (g, h) PBBT-BDS.

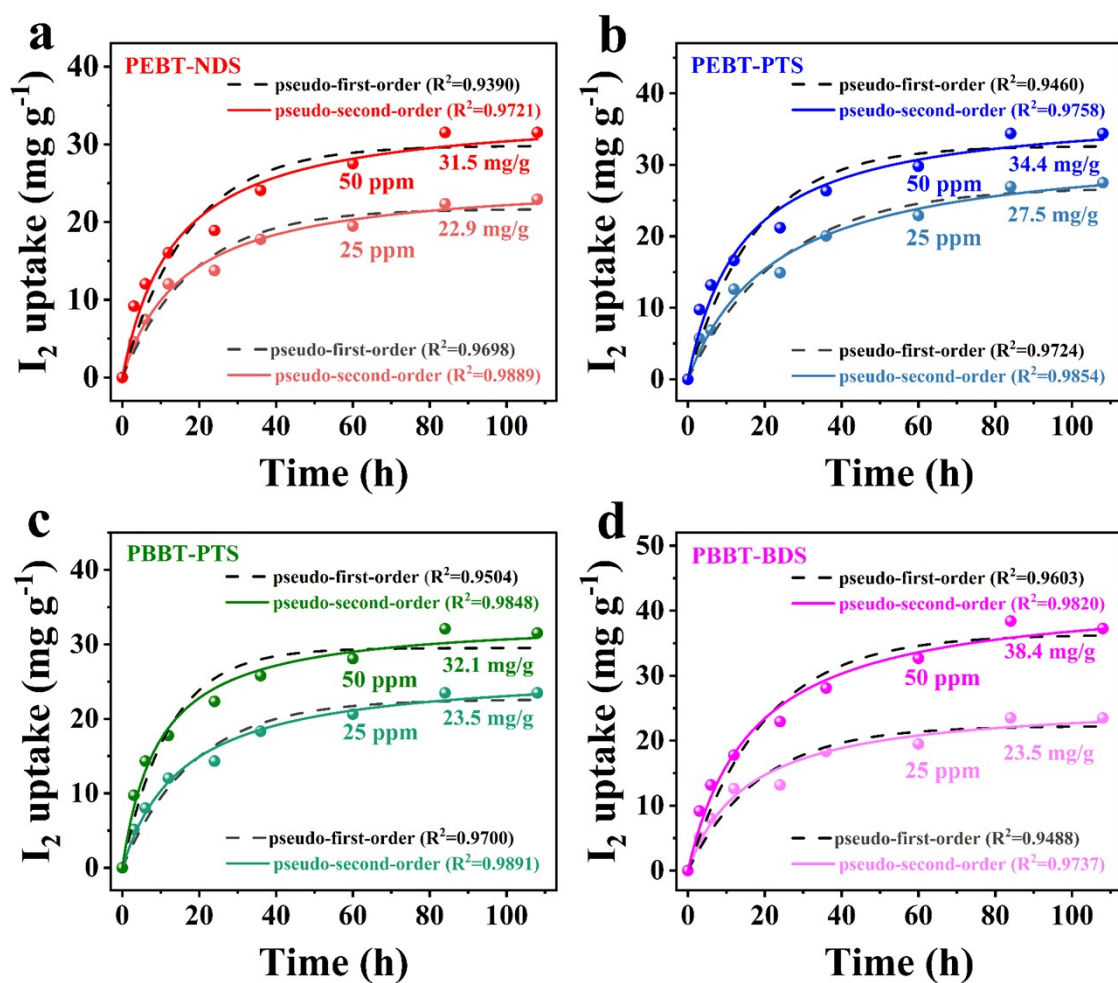


Figure S8. Adsorption of iodine in different concentrations of iodine-cyclohexane belongs to the time and corresponding dynamic fitting curve of (a) PEBT-NDS, (b) PEBT-PTS, (c) PBBT-PTS, (d) PBBT-BDS.

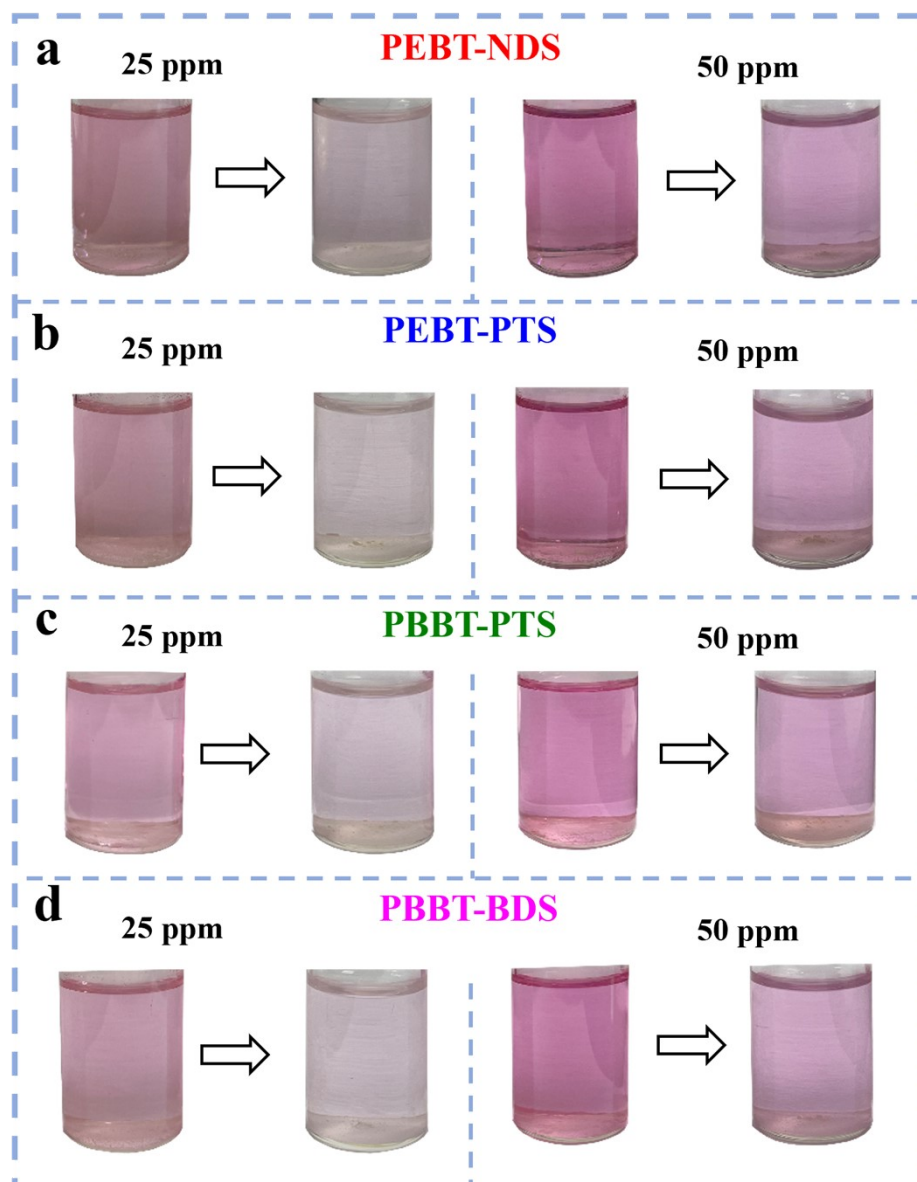


Figure S9. Photos of iodine-cyclohexane before and after adsorption of four IOCs of (a) PEBT-NDS, (b) PEBT-PTS, (c) PBBT-PTS, (d) PBBT-BDS.

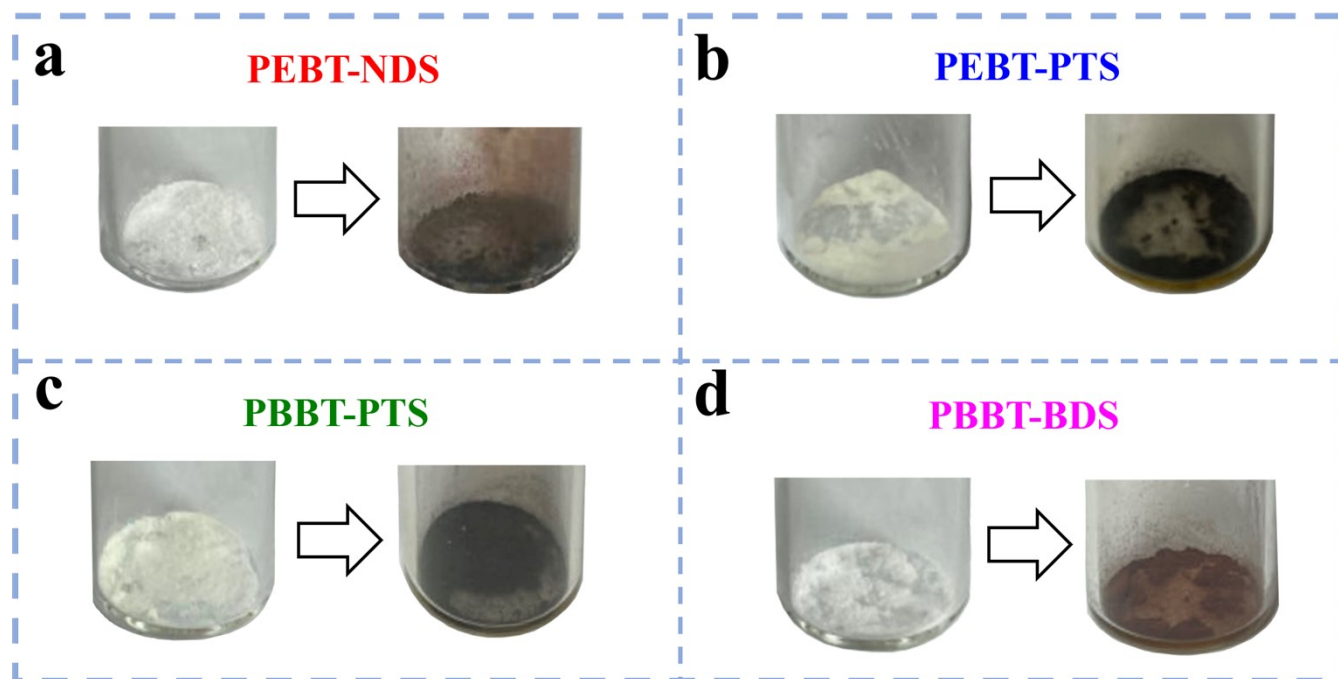


Figure S10. Photos of four IOCs before and after iodine vapor adsorption of (a) PEBT-NDS, (b) PEBT-PTS, (c) PBBT-PTS, (d) PBBT-BDS.

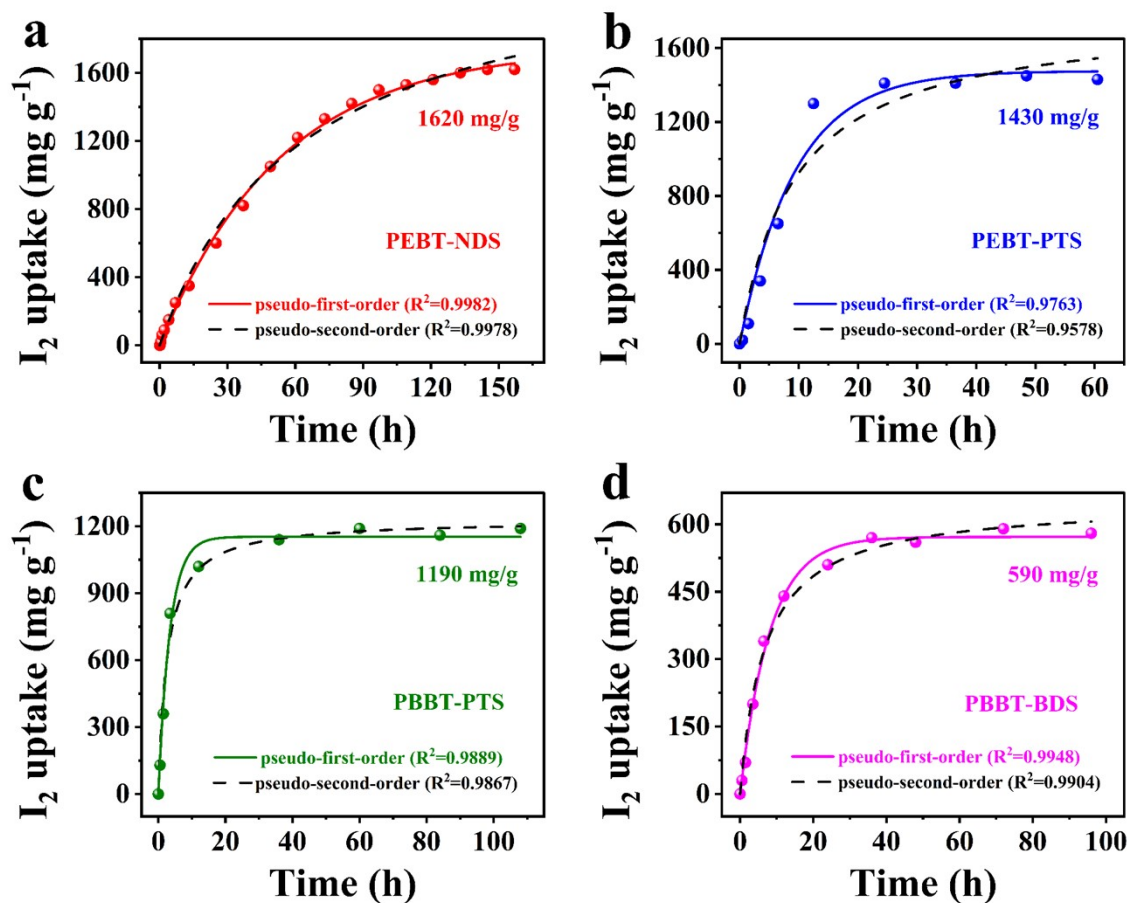


Figure S11. Iodine adsorption in iodine vapor belongs to the time at 70 °C and their corresponding dynamic fitting curve of (a) PEBT-NDS, (b) PEBT-PTS, (c) PBBT-PTS, (d) PBBT-BDS.

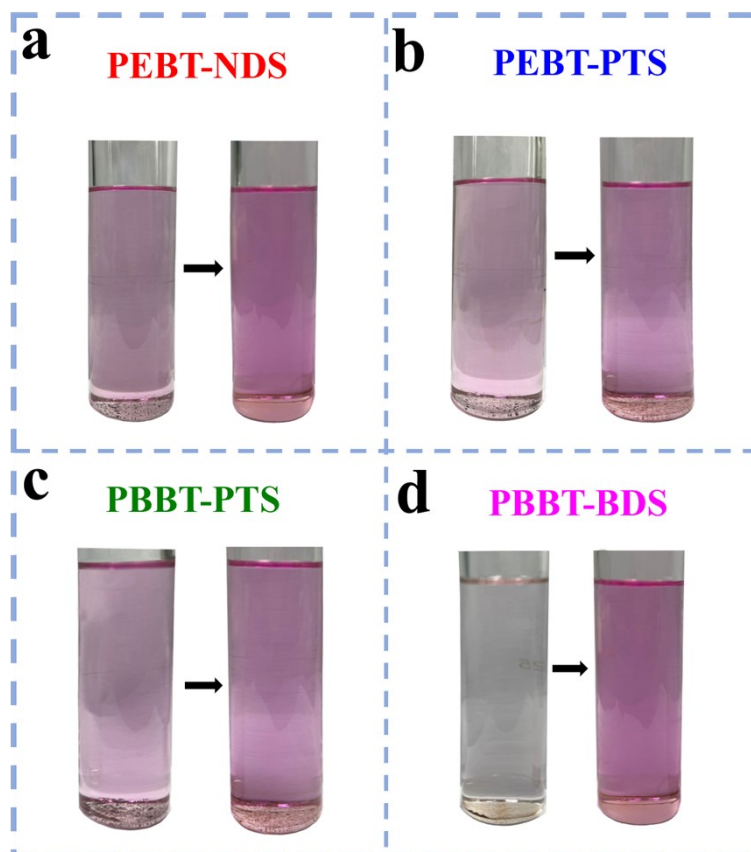


Figure S12. Photos of four IOCs before and after iodine release in cyclohexane of (a) PEBT-NDS, (b) PEBT-PTS, (c) PBBT-PTS, (d) PBBT-BDS.

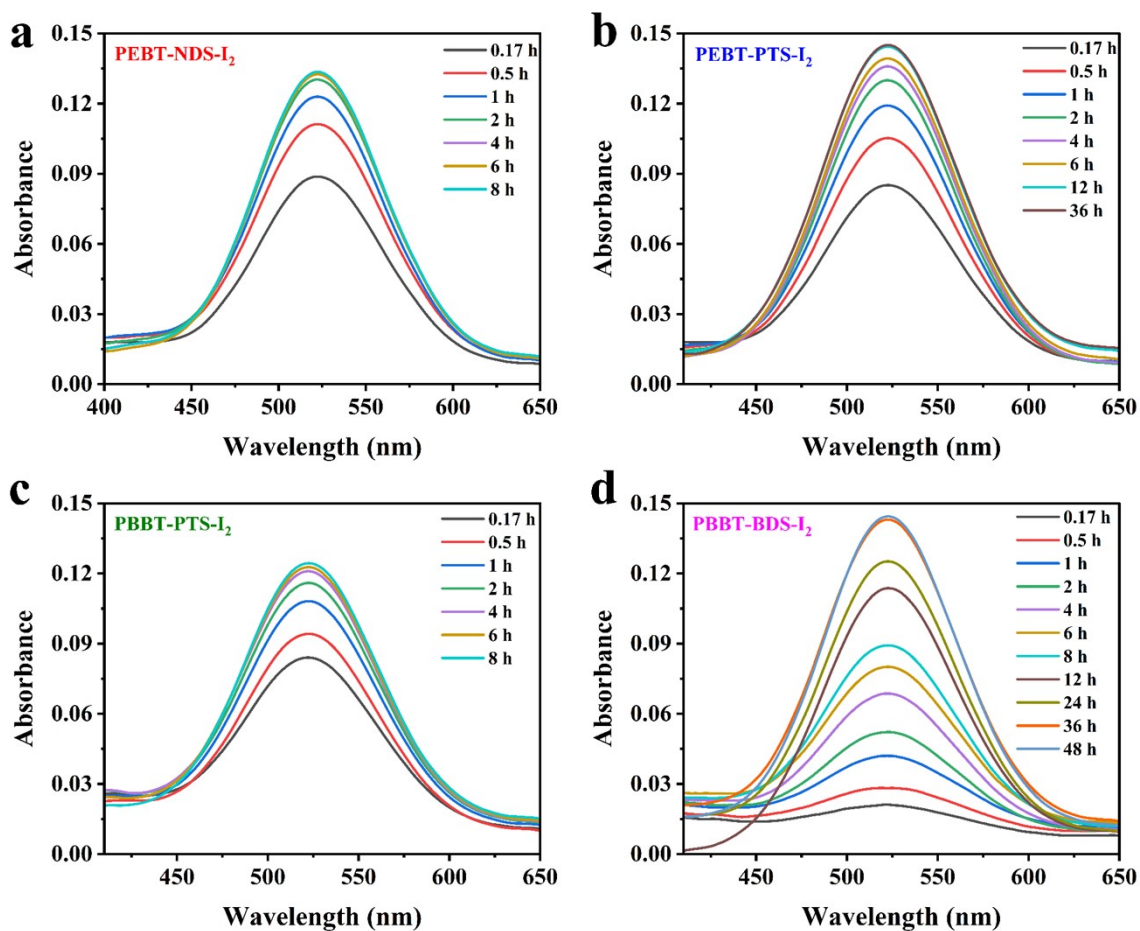


Figure S13. UV-Vis absorption curves of release in cyclohexane of (a) PEBT-NDS, (b) PEBT-PTS, (c) PBBT-PTS, (d) PBBT-BDS.

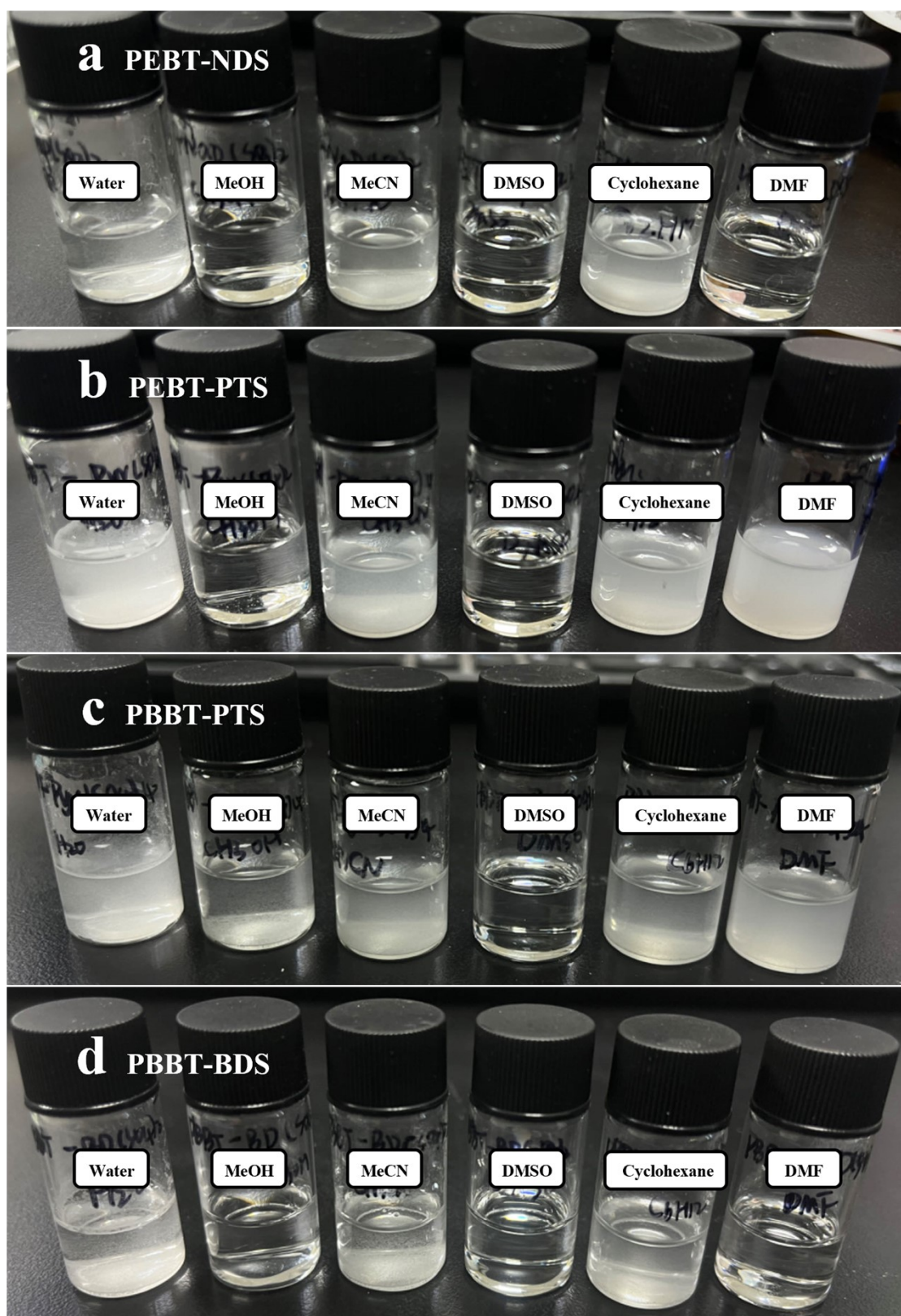


Figure S14. Photos of solubility of four IOCs in different solvents at 70 °C.

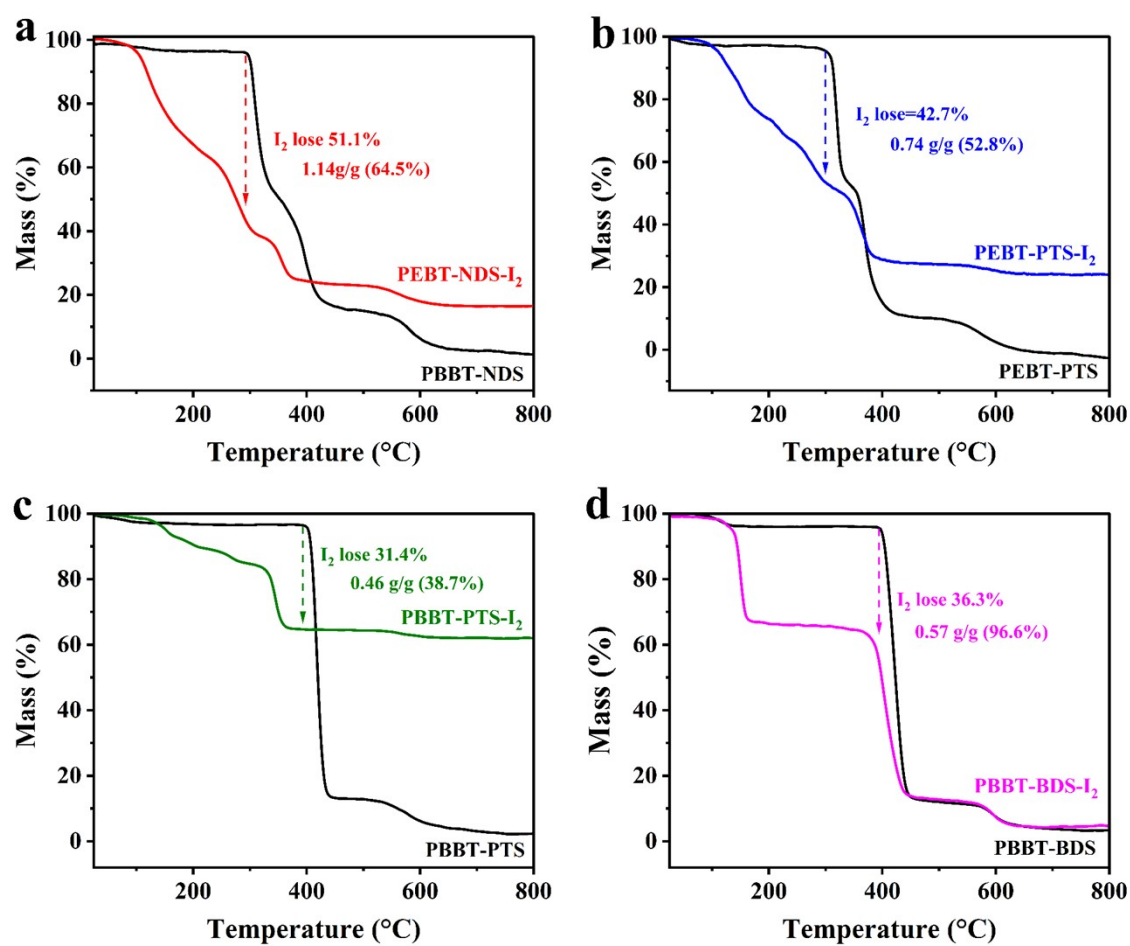


Figure S15. TGA curve of four IOCs before and after iodine adsorption of (a) PEBT-NDS, (b) PEBT-PTS, (c) PBBT-PTS, (d) PBBT-BDS.

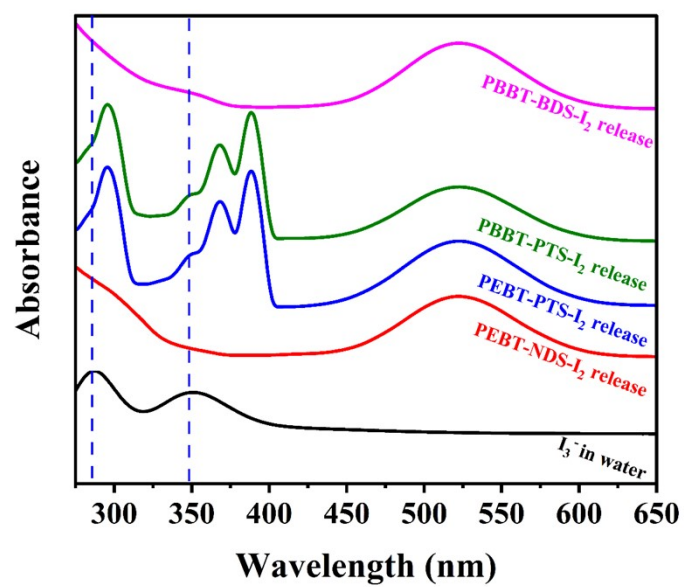


Figure S16. UV-Vis absorption curves of four IOCs release in cyclohexane after iodine adsorption and I_3^- in water.

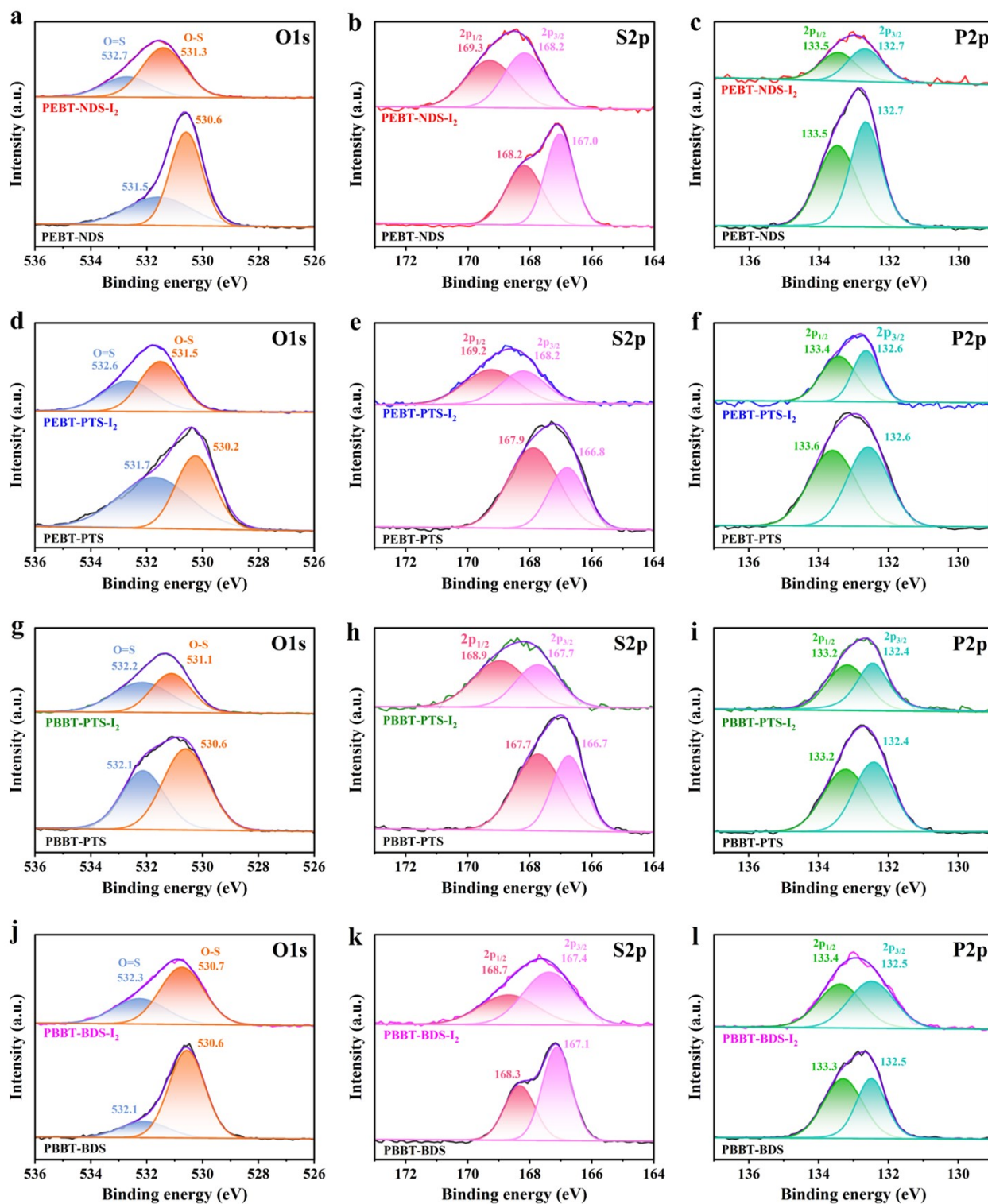


Figure S17. XPS high-resolution spectrum of four IOC materials before and after iodine adsorption of (a-c) PEBT-NDS, (d-f) PEBT-PTS, (g-i) PBBT-PTS, (j-l) PBBT-BDS.

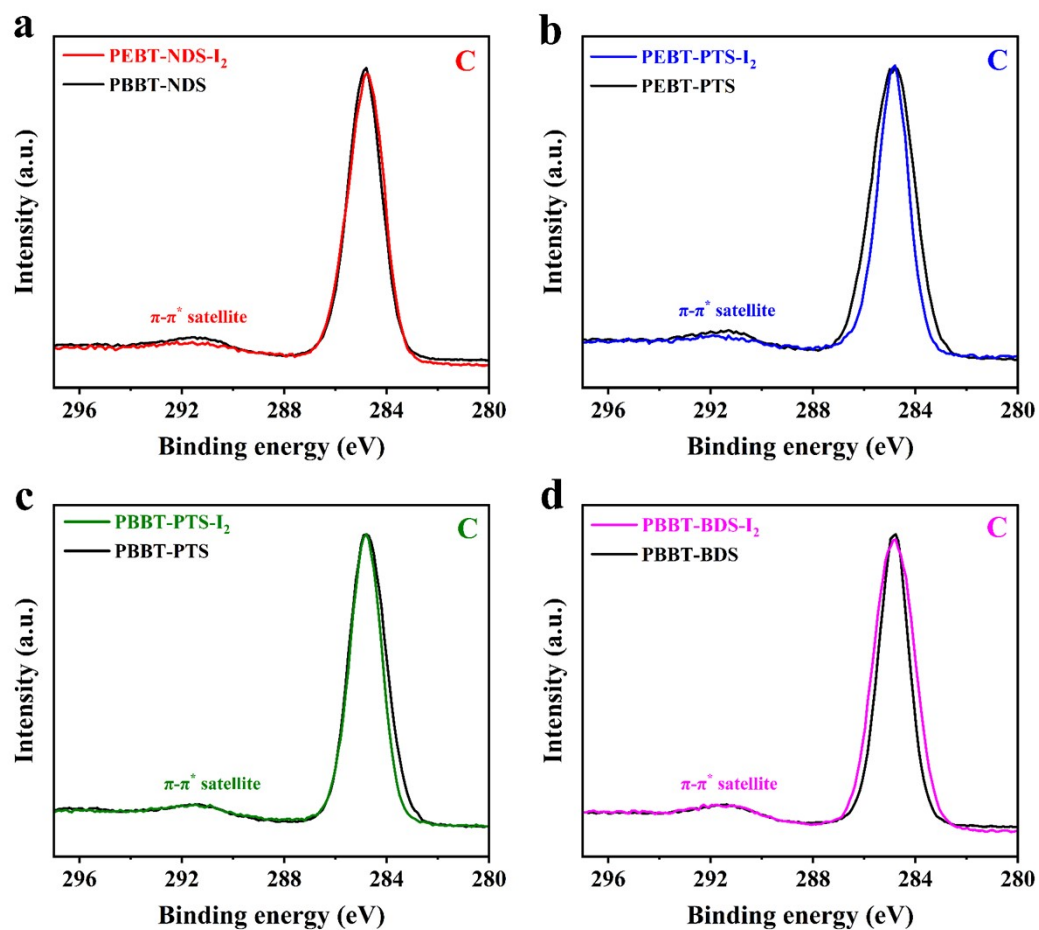


Figure S18. XPS C high-resolution spectrum of four IOCs before and after iodine adsorption of (a) PEBT-NDS, (b) PEBT-PTS, (c) PBBT-PTS, (d) PBBT-BDS.

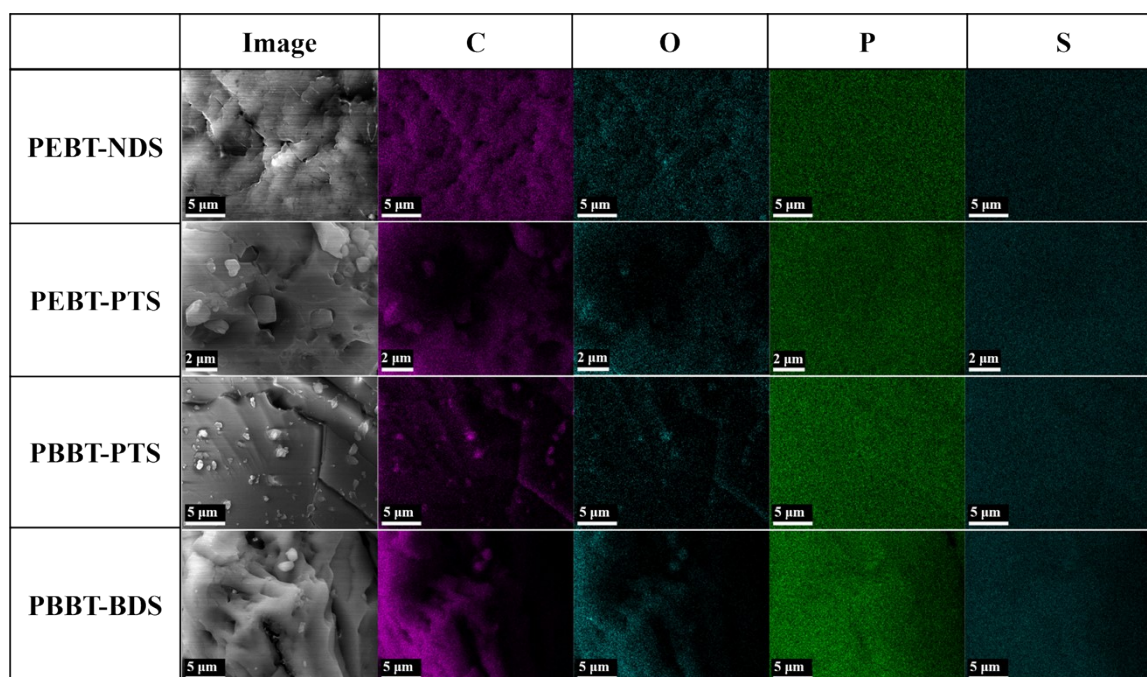


Figure S19. Element distribution mapping of four IOCs.

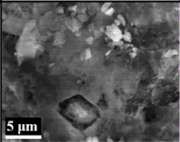
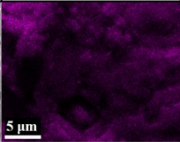
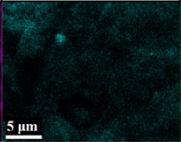
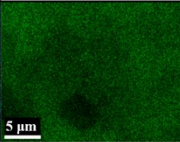
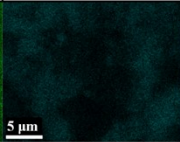
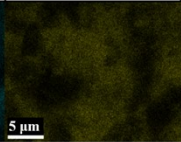
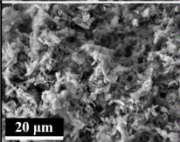
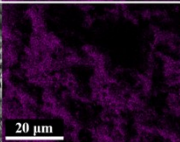
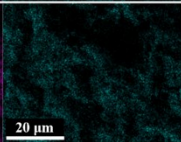
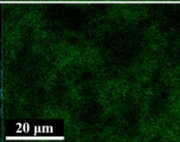
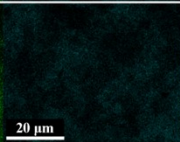
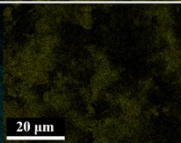
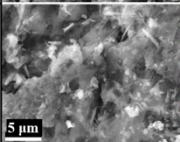
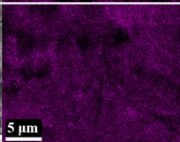
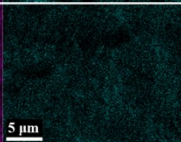
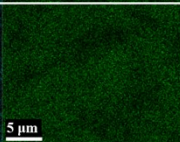
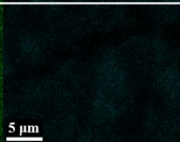
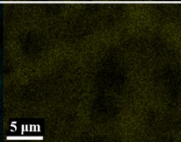
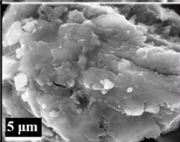
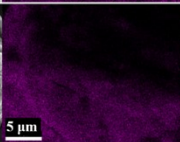

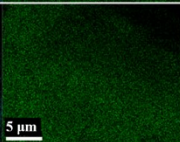

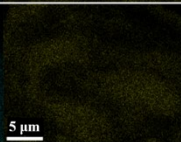
	Image	C	O	P	S	I
PEBT-NDS						
PEBT-PTS						
PBBT-PTS						
PBBT-BDS						

Figure S20. Element distribution mapping of four IOCs after iodine adsorption.

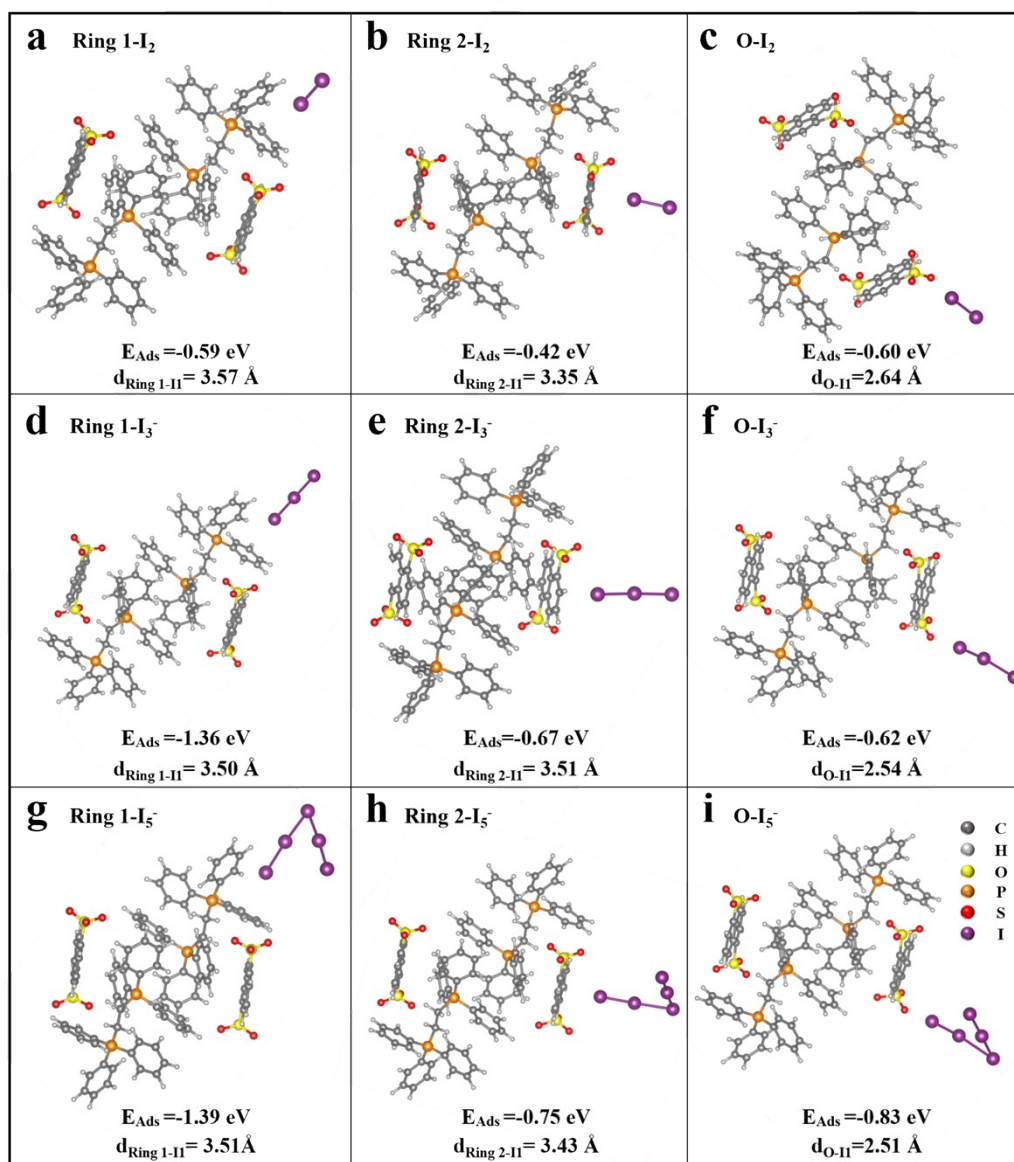


Figure S21. The lowest energy configurations, adsorption energies, and distances of (a-c) ring 1 of PEPT, ring 2 and O of NDS on I₂ sites, (d-f) ring 1 of PEPT, ring 2 and O of NDS on I₃⁻ sites, (g-h) ring 1 of PEPT, ring 2 and O of NDS on I₅⁻ sites.

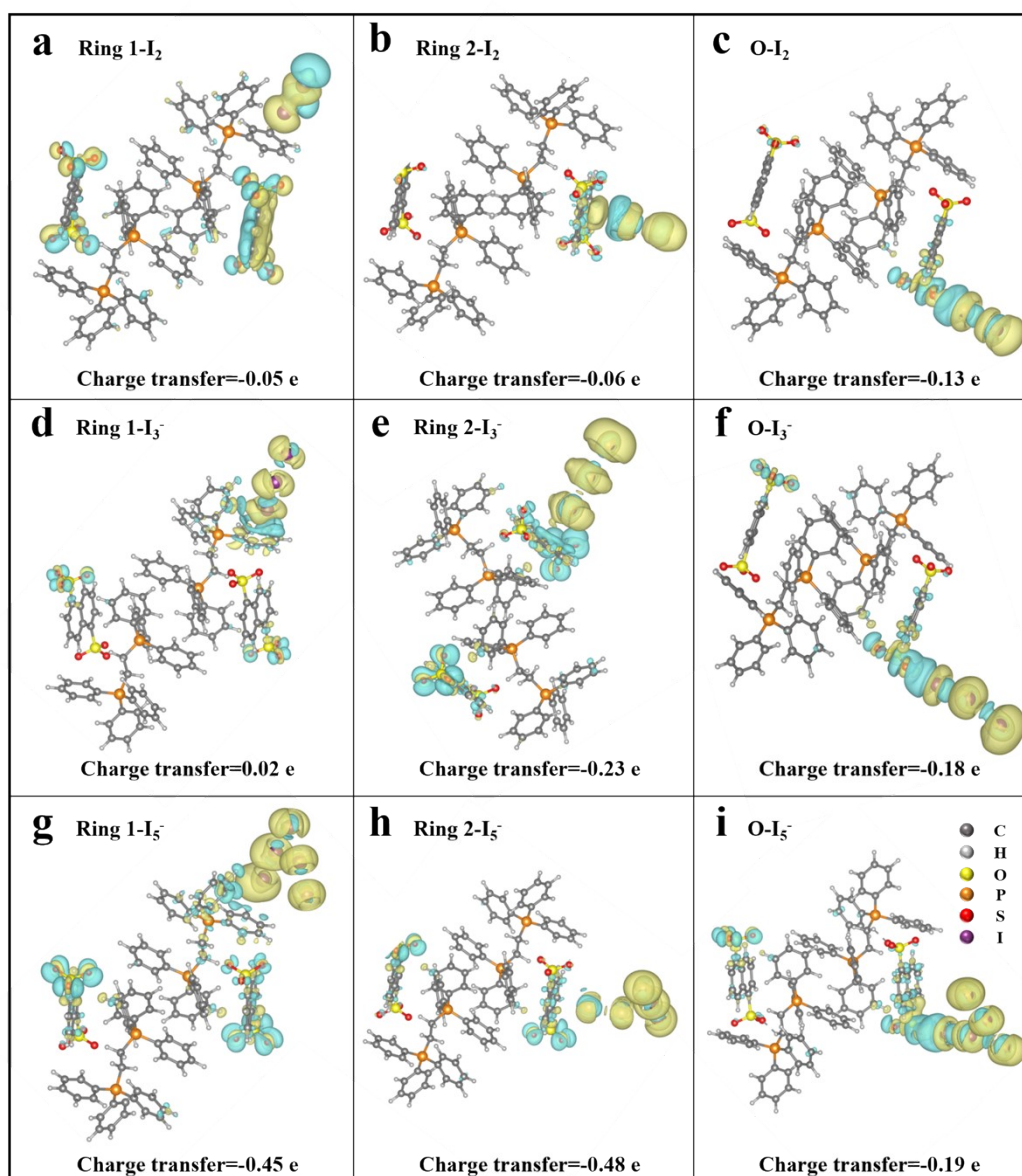


Figure S22. Charge transfer diagrams of (a-c) ring 1 of PEBT, ring 2 and O of NDS on I₂ sites, (d-f) ring 1 of PEBT, ring 2, and O of NDS on I₃⁻ sites, (g-h) ring 1, ring 2, and O of NDS on I₅⁻ sites.

Table S1. Preparation parameters of four IOCs.

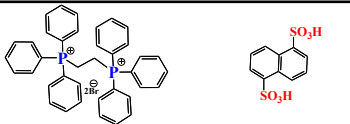
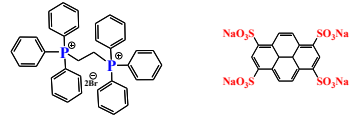
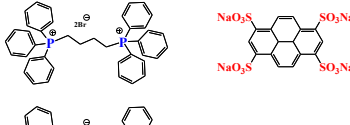
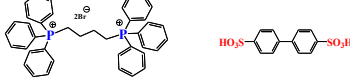
Monomer structural formula	Name of single crystal	Cationic monomer and dosage	Anionic monomer and dosage	Morphology
	PEBT-NDS	PEBT (0.1 mmol)	NDS (0.1 mmol)	Colourless rhombus
	PEBT-PTS	PEBT (0.1 mmol)	PTS (0.05 mmol)	Pale yellow quadrate
	PBBT-PTS	PBBT (0.1 mmol)	PTS (0.05 mmol)	Pale yellow hexagon
	PBBT-BDS	PBBT (0.1 mmol)	BDS (0.1 mmol)	Colorless rod

Table S2. Unit cell packing of four IOCs.

Single crystal	a	b	c	α	β	γ	Volume	Crystal system	Point group	Space group
PEBT-NDS	9.2113	13.5991	17.3584	98.176	93.192	106.950	2047.9	Triclinic system	$\bar{1}$	$P\bar{1}$
PEBT-PTS	11.9946	20.2180	17.2493	90	99.561	90	4125.0	Monoclinic system	2/m	$P2_1/n$
PBBT-PTS	13.4375	19.787	18.4255	90	106.827	90	4689.4	Monoclinic system	2/m	$P2_1/n$
PBBT-BDS	10.5835	14.1726	17.216	70.458	77.061	71.936	2292.7	Triclinic system	$\bar{1}$	$P\bar{1}$

Table S3. Plane angle of benzene rings of PEBT and PBBT in four IOCs.

Plane angle	∠Ring 1	∠Ring 1	∠Ring 2	∠Ring 4	∠Ring 4	∠Ring 5
	&Ring 2	&Ring 3	&Ring 3	&Ring 5	&Ring 6	&Ring 6
PEBT in PEBT-NDS	63.04°	69.35°	87.68°	57.90°	66.29°	73.19°
PEBT in PEBT-PTS	77.92°	76.92°	58.14°	57.52°	78.67°	63.55°
PBBT in PBBT-PTS	73.77°	67.45°	60.34°	79.88°	60.40°	79.18°
PBBT in PBBT-BDS	84.42°	83.72°	60.75°	50.98°	85.26°	62.95°

Table S4. Solubleness of four IOCs in different solvents at 70 °C.

	Water	MeOH	MeCN	DMSO	Cyclohexan e	DMF
PEBT-NDS	×	√	×	√	×	√
PEBT-PTS	×	√	×	√	×	×
PBBT-PTS	×	×	×	√	×	×
PBBT-BDS	×	√	×	√	×	√

Table S5. EDS data of four IOCs.

Atomic (%)	PEBT-NDS	PEBT-PTS	PBBT-PTS	PBBT-BDS
C K	81.91	82.80	81.31	84.57
O K	12.43	9.23	6.24	9.23
P K	2.99	4.26	6.58	3.36
S K	2.67	3.70	5.87	2.83

Table S6. EDS data of four IOCs after iodine adsorption.

Atomic (%)	PEBT-NDS	PEBT-PTS	PBBT-PTS	PBBT-BDS
C K	79.73	74.37	79.62	83.11
O K	6.02	11.88	7.65	9.18
P K	4.46	3.28	3.66	3.04
S K	3.65	4.28	2.80	2.53
I L	6.15	6.18	6.27	2.15

Table S7. The distance between iodine atoms.

Site	I ₂	I ₃ ⁻		I ₅ ⁻			
	I1-I2	I1-I2	I2-I3	I1-I2	I2-I3	I3-I4	I4-I5
Ring 1	2.80	2.93	2.89	2.85	3.02	3.08	2.80
Ring 2	2.69	2.85	2.91	2.76	3.09	3.04	2.82
O	2.75	2.82	2.96	2.74	3.74	2.98	2.85

Table S8. Comparison with other reported iodine vapor adsorption properties and synthesis conditions.

Adsorbent ^[a]	Adsorption capacity of iodine vapor (g g ⁻¹)	Adsorption temperature (°C)	Adsorption time (h)	Synthesis temperature ^[b]	Reaction time	Ref.
PEBT-NDS	1.62	70	144	RT	12 h	This work
BPy-Cage	3.23	75	14	RT	12 h	[10]
Etp6β	0.25	85	1	RT	12 h	[46]
COF-TpgBD	1.81	125	~3 d	7 °C	72 h	[54]
NACs-TPAPyH	1.27	70	20	RT	-	[55]
UiO-66-NH-TD	1.33	75	2.5	120 °C	24 h	[56]
COFs@cotton	0.53	77	7	RT	-	[57]
BPy-Box·4Cl	3.99	75	~15	Methanol reflux	96 h	[58]
TJNU-203	5.885	77	120	120 °C	72 h	[59]
SCU-SnS	6.12	75	120	180 °C	96 h	[60]

^[a] BPy-Cage: bipyridine-based nonporous adaptive cage; Etp6β: *per*-ethylated pillar[6]arene; COF: Covalent organic framework, Tpg: 2,4,6-Trihydroxylbenzene-1,3,5-tricarbaldehyde, BD: benzidine; NACs-TPAPyH: 4-(4-(diphenylamino)phenyl)pyridin-1-ium chloride; UiO-66-NH₂: from ZrCl₄ and 2-aminoterephthalic acid; COF: from 1,3,5-tris(4-aminophenyl)benzene and terephthalaldehyde; BPy-Box·4Cl: a tetracationic cyclophane composed of two 3,3'-bipyridinium units linked together by two *p*-xylylene bridges; TJNU-203: 2D COF from 1,3,5-trimethyl-2,4,6-tris(4-aminophenyl) benzene (TMTAPB) and terephthalaldehyde (TPA); SCU-SnS: A metal-sulfide framework ((NH₄)₂(Sn₃S₇)).

^[b] RT: Room temperature.

References

1. E. D. Revellame, D. L. Fortela, W. Sharp, R. Hernandez and M. E. Zappi, Adsorption kinetic modeling using pseudo-first order and pseudo-second order rate laws: A review, *Clean Eng. Technol.*, 2020, **1**, 100032.
2. Y. Gao, Y. Huo, M. Chen, X. Su, J. Zhan, L. Wang, F. Liu, J. Zhu, Y. Zeng, J. Fan, Z. Li, R. Chen and H.-L. Wang, Phenolic based porous carbon fibers with superior surface area and adsorption efficiency for radioactive protection, *Adv. Fiber Mater.*, 2023, **5**, 1431-1446.
3. G. Kresse and J. Furthmüller, Efficient iterative schemes for ab initio total-energy calculations using a plane-wave basis set, *Phys. Rev. B*, 1996, **54**, 11169-11186.
4. G. Kresse and J. Furthmüller, Efficiency of ab-initio total energy calculations for metals and semiconductors using a plane-wave basis set, *Comp. Mater. Sci.*, 1996, **6**, 15-50.
5. G. Kresse and J. Hafner, Ab initio molecular dynamics for liquid metals, *Phys. Rev. B*, 1993, **47**, 558-561.
6. J. P. Perdew, K. Burke and M. Ernzerhof, Generalized gradient approximation made simple, *Phys. Rev. Lett.*, 1996, **77**, 3865-3868.
7. S. Grimme, J. Antony, S. Ehrlich and H. Krieg, A consistent and accurate ab initio parametrization of density functional dispersion correction (DFT-D) for the 94 elements H-Pu, *J. Chem. Phys.*, 2010, **132**.
8. S. Grimme, S. Ehrlich and L. Goerigk, Effect of the damping function in dispersion corrected density functional theory, *J. Comput. Chem.*, 2011, **32**, 1456-1465.
9. G. Henkelman, A. Arnaldsson and H. Jonsson, A fast and robust algorithm for Bader decomposition of charge density, *Comp. Mater. Sci.*, 2006, **36**, 354-360.